Alteration of the premature tRNA landscape by gammaherpesvirus infection

Jessica Tucker[1], Aaron M. Schaller[2], Ian Willis[3], and Britt A. Glaunsinger[1,2,4*]

[1]Department of Plant and Microbial Biology, University of California Berkeley, CA, USA
[2]Department of Molecular and Cell Biology, University of California Berkeley, CA, USA
[3]Departments of Biochemistry and Systems and Computational Biology, Albert Einstein College of Medicine, Bronx NY, USA
[4]Howard Hughes Medical Institute, University of California Berkeley, CA, USA
*Address correspondence to: Britt Glaunsinger, glaunsinger@berkeley.edu

Abstract

Transfer RNAs (tRNAs) are transcribed by RNA polymerase III (RNAPIII) and play a central role in decoding our genome. Many DNA tumor viruses enhance the activity of RNAPIII, yet whether infection alters tRNA expression is largely unknown. Here, we present the first genome wide analysis of how viral infection alters the tRNAome. Using a tRNA-specific sequencing method (DM-tRNA-seq), we find that the murine gammaherpesvirus MHV68 induces global changes in pre-tRNA expression, indicating that differential tRNA gene induction is a characteristic of DNA virus infection. Elevated pre-tRNA expression corresponds to increased RNAPIII occupancy, but post-transcriptional mechanisms also contribute. Pre-tRNA accumulation, but not RNAPIII recruitment, requires the virally encoded mRNA endonuclease muSOX, suggesting interplay between the different facets of virus-induced gene regulation. Collectively, these findings reveal pervasive changes to tRNA expression during DNA virus infection and highlight the potential of using viruses to explore tRNA biology.

Impact

The first genome-wide analysis of virus-induced tRNA expression changes reveals that tRNA transcription and processing are perturbed by the gammaherpesvirus MHV68.

30 **Introduction**

31 The elegant design of the tRNA decoder, an adaptor molecule which converts genetic
32 information into protein, was proposed over 60 years ago (1). Although tRNAs were the first
33 non-coding RNA described, our understanding of tRNA biology, especially their functions
34 outside of protein translation and what dictates their expression, remains limited. This is partly
35 due to the difficulties in applying RNA sequencing and analysis platforms to tRNAs, but recent
36 methodological advances have resulted in a surge of new studies that help to resolve these
37 complexities (2-4). Non-canonical functions of tRNA transcripts have been described, namely
38 the discovery that both premature and mature tRNAs undergo fragmentation into shorter RNAs
39 with numerous regulatory functions in response to stress, cancer, and viral infection (reviewed
40 in (5, 6)). Given the evidence that the ~400 predicted tRNA genes in mammalian genomes are
41 differentially expressed across cell lines (7-9) and that viral infection can lead to post-
42 transcriptional modulation of tRNAs (10, 11), defining the tRNAome under varying conditions will
43 be central to our understanding of tRNA function, canonical and otherwise.

44 RNA polymerase III (RNAPIII) transcribes tRNA genes and exhibits enhanced activity
45 during infection with DNA viruses (12-17), many of which encode their own RNAPIII genes.
46 Though RNAPIII activation stimulates expression of viral RNAPIII genes, concomitant
47 accumulation of host RNAPIII transcripts can trigger antiviral immune responses. For example,
48 the induction or misprocessing of RNAPIII-generated host 5S RNA pseudogene and vault RNA
49 transcripts during Herpes Simplex Virus-1 (HSV-1) and Kaposi's sarcoma-associated
50 herpesvirus (KSHV) infection, respectively, activates RNA sensing pattern recognition receptors
51 (18, 19). The RNAPIII-driven B2 SINE family of retrotransposons are also induced and sensed
52 during infection with the murine gammaherpesvirus MHV68, although MHV68 has uniquely
53 evolved to hijack components of the antiviral NF-κB signaling pathway to instead promote viral
54 gene expression and replication (20-24). While it is clear that induced RNAPIII transcripts can
55 have functional consequences during infection, little is known about the mechanisms underlying

56 the selectivity of RNAPIII activation, including identification of the specific RNAPIII genes
57 induced by viral infection on a genome-wide scale.

58 DNA viruses upregulate RNAPIII transcription by increasing the abundance of limiting
59 RNAPIII transcription factor complexes specific for certain RNAPIII promoter types (reviewed in
60 (25)). RNAPIII genes have one of three different promoters that recruit a unique combination of
61 the transcription factor complexes, TFIIIA (Gtf3a), TFIIIB (TBP, Brf1 or Brf2, and Bdp1), TFIIIC
62 (Gtf3c1-6) or SNAPc (Snapc1-5) plus RNAPIII for gene expression (26). tRNAs use the
63 abundant RNAPIII promoter type II, which consists of internal A and B boxes that bind TFIIIC
64 and ultimately recruit TFIIIB and RNAPIII to initiate transcription. 7SL, short interspersed nuclear
65 elements (SINEs), vault RNAs, and viral RNAPIII genes also use type II promoters. 5S rRNA
66 genes have an internal type I promoter, which binds TFIIIA (Gtf3a) and requires TFIIIC, TFIIIB,
67 and RNAPIII for transcription. In contrast, type III promoters found in U6 and 7SK genes have
68 external promoters that are TFIIIC-independent and bind the SNAPc complex and a unique
69 TFIIIB complex containing Brf2 protein, rather than Brf1. Defining virally-induced RNAPIII
70 transcript classes and/or transcription factor complexes has been essential for understanding
71 how viruses enhance RNAPIII activity.

72 The breadth of tRNA function in cells and the fact that many DNA viruses increase
73 RNAPIII activity suggest that regulation of tRNA expression may be a significant point of control
74 during infection. The repertoire of differentially expressed tRNA genes during DNA virus
75 infection is not known, although individual tRNA transcripts are upregulated during EBV and
76 SV40 infection (12, 27). Here, we present the first genome-wide analysis of how infection alters
77 tRNA abundance using the model gammaherpesvirus MHV68. Using a tRNA-specific
78 sequencing method (DM-tRNA-seq) and analysis pipeline, we found that lytic MHV68 infection
79 leads to a $\geq$3-fold increase in pre-tRNA levels for approximately 14% of tRNA genes. Notably,
80 infection-induced pre-tRNAs do not appear to undergo canonical maturation, as mature tRNA
81 levels remain largely constant. The accumulation of pre-tRNAs occurs through a combination of

82 transcriptional induction, as evidenced by increased RNAPIII occupancy at activated loci, and
83 post-transcriptional mechanisms. In particular, pre-tRNA accumulation is linked to the activity of
84 the viral endonuclease muSOX/ORF37, which cleaves host mRNAs and downregulates protein
85 synthesis during infection in a process called host shutoff. Given that muSOX is not required for
86 RNAPIII recruitment to tRNA genes, we instead hypothesize that degradation of host mRNAs
87 depletes factors involved in tRNA processing and turnover, contributing to the accumulation of
88 pre-tRNAs. The alterations in tRNA expression during MHV68 infection described here highlight
89 the potential of using viruses to explore mechanistic details of tRNA maturation and turnover.
90

91 **Results**

92 **Pre-tRNAs increase in abundance in MHV68-infected cells**

93 Given that MHV68 infection upregulates RNAPIII-driven B2 SINEs (20), which are
94 evolutionarily related to tRNAs, we hypothesized that gammaherpesviral infection may also alter
95 cellular tRNA expression. We first measured pre-tRNA levels by RT-qPCR, using primer sets
96 that were specific for premature tRNAs (pre-tRNAs) produced from intron-containing tRNA-Tyr
97 and tRNA-Leu genes (Figure 1A). During MHV68 infection of NIH3T3 mouse fibroblasts, pre-
98 tRNA levels increased by greater than 15-fold (Figure 1A). This induction appeared specific to
99 tRNAs, as other RNAPIII transcripts (*7SK*, *U6*, *5S*, and *7SL*) did not show differential expression
100 during infection. This is in contrast to Epstein-Barr virus, a gammaherpesvirus that is associated
101 with increased expression of many RNAPIII gene classes due to upregulation of TFIIIB/TFIIIC
102 transcription factor complex subunits at both the mRNA and protein level (12). Accordingly, we
103 did not detect changes in TFIIIB/C subunit mRNA levels upon MHV68 infection (Supplemental
104 Figure 1), and in fact these transcripts were less abundant during infection. This is in line with
105 the general downregulation of host mRNA transcripts that occurs during MHV68-induced host
106 shutoff (28). A time course of MHV68 infection showed that pre-tRNA-Tyr and pre-tRNA-Leu
107 levels were increased by 12 hours post infection (hpi), with their levels accumulating through

108 late stages of infection at 24 hpi (Figure 1B). Notably, the timing of pre-tRNA induction
109 corresponded well with the induction pattern for B2 SINEs. Finally, we also confirmed that pre-
110 tRNA-Tyr and pre-tRNA-Leu are upregulated by northern blot, a method that does not rely on
111 cDNA production (Figure 1C). Mature tRNA-Tyr transcript levels remained constant during
112 infection, suggesting that infection-induced pre-tRNAs may not be processed into mature
113 tRNAs.

114 Given the kinetics of induction, we hypothesized that events occurring mid to late
115 infection were responsible for pre-tRNA accumulation, as opposed to a cellular response to viral
116 binding and entry. In agreement with this hypothesis, infection of MC57G fibroblasts with UV-
117 inactivated MHV68 did not lead to pre-tRNA-Tyr induction (Figure 1D). Additionally, wild type
118 MHV68 infection of the MC57G fibroblast cell line led to an induction similar to NIH3T3s. UV-
119 inactivation prevented post-entry viral gene expression, as demonstrated by the absence of
120 expression of the immediate early viral gene ORF50. To narrow down the gene class
121 responsible for the kinetics of tRNA induction, we performed infections in the presence of
122 phosphonoacetic acid (PAA), which blocks viral DNA replication and prevents the expression of
123 viral late genes, such as gB. Although late gene expression was inhibited, pre-tRNA-Tyr
124 accumulated to similar levels in cells infected in the presence of PAA (Figure 1E). Thus, one or
125 more effects of early viral gene expression underlie pre-tRNA accumulation during MHV68
126 infection. Together, these data demonstrate that early viral gene expression drives the
127 increased abundance of host pre-tRNAs.

128

129 **Dm-tRNA-seq reveals upregulation of premature tRNAs during infection**

130 Extensive base modification of tRNAs can prevent reverse transcription of full-length
131 cDNA products. Although there are some modifications present in pre-tRNAs, they likely have
132 not undergone extensive modification and therefore are more efficiently amplified relative to
133 mature tRNAs during reverse transcription (4, 29). Amplification of full-length cDNA products

134 from tRNAs can be improved by using the highly processive thermostable group II-intron

Figure 1

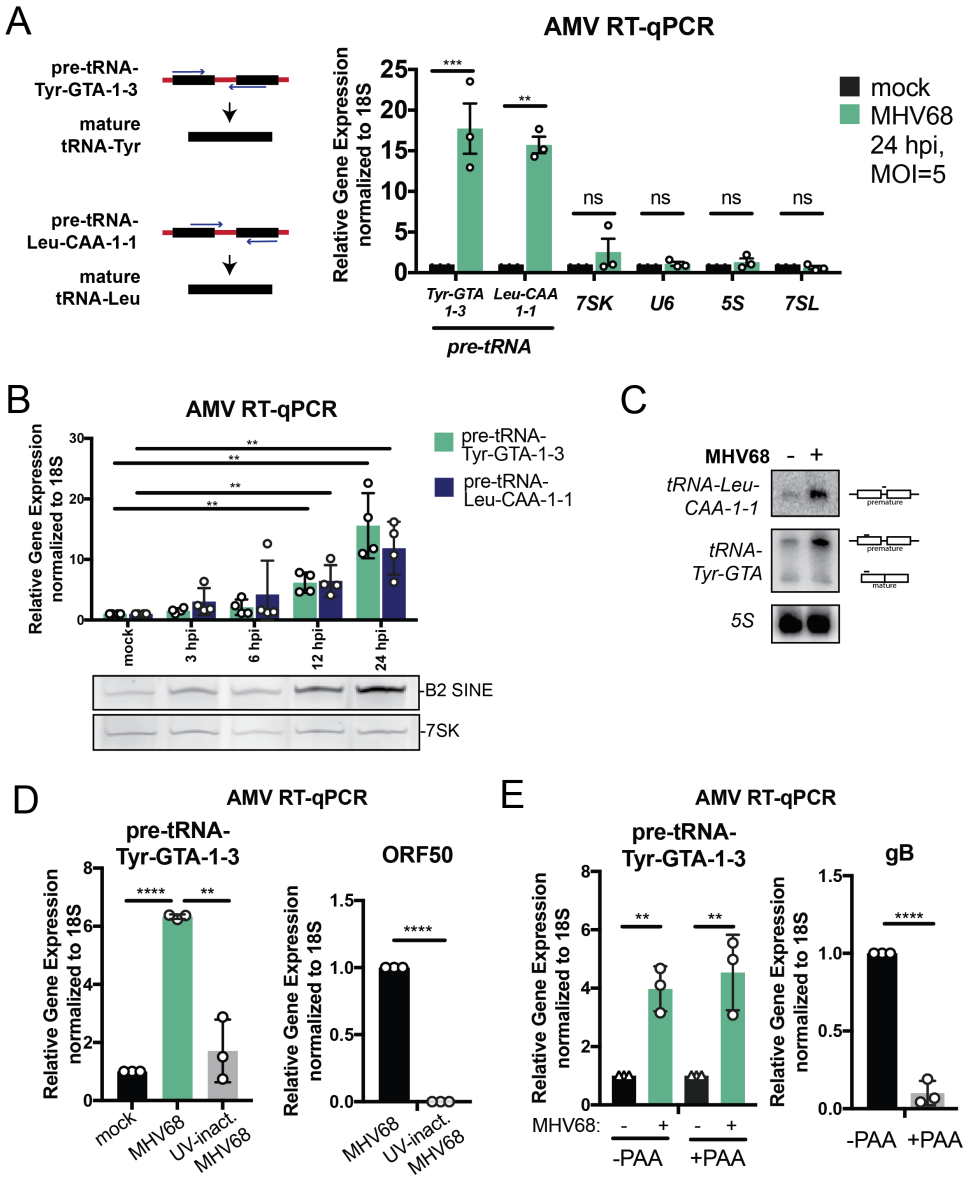

Figure 1. MHV68 infection results in increased pre-tRNA expression.
(A) Pre-tRNA-Tyr-GTA-1-3 and pre-tRNA-Tyr-Leu-CAA-1-1 are transcribed with flanking and intron sequences (depicted in red), which are removed during maturation. Pre-tRNAs were detected with forward or reverse primers with 3' ends complementary to the intron by AMV RT-qPCR. Relative abundance of pre-tRNAs and other RNAPIII transcripts was measured by RT-qPCR in mock and MHV68-infected NIH3T3s. Expression was normalized to 18S rRNA and compared to values from mock-infected cells. (B) RNA was extracted from NIH3T3 cells following a time course of MHV68 infection and used for both AMV RT-qPCR to detect pre-tRNAs and primer extension to detect B2 SINE and 7SK transcripts. (C) Northern blot was performed on RNA from mock or MHV68-infected MC57Gs. Transcripts produced from tRNA-Leu-CAA-1-1 were detected with intron and exon-specific probes. tRNA-Tyr transcripts were detected with a probe that anneals with a conserved 5' region in the tRNA-Tyr family. Probe binding is depicted on the right. (E) RNA from mock and MHV68-infected MC57Gs +/- UV-inactivation was used for AMV RT-qPCR. ORF50 is an early viral gene. (F) Mock and MHV68-infected MC57Gs were treated with 200 ng/l phosphonoacetic acid (PAA) to block viral DNA replication, and extracted RNA was used for RT-qPCR analysis. gB is a late viral gene whose expression is dependent on successful viral DNA replication. All infections were done at an MOI=5 for 24 hours unless otherwise noted. RT-qPCR experiments were done in triplicate at a minimum. Error bars show SD and statistics were calculated using an unpaired t- test. *P<0.05, **P<0.01. ***P<0.001.

135

136 containing reverse transcriptase (TGIRT) (30) and by partial removal of tRNA strong-stop

137 modifications by treating with AlkB demethylases (2, 3). To define the extent of tRNA

138 upregulation genome-wide, we therefore generated sequencing libraries using TGIRT and AlkB-
139 treated small RNA (a method called DM-tRNA-seq (3)) in mock versus MHV68 infected MC57G
140 cells. Our analysis pipeline was designed to distinguish reads from pre-tRNAs and mature
141 tRNAs, as our preliminary data with tRNA-Leu and tRNA-Tyr suggested that MHV68 may
142 elevate pre-tRNA but not mature tRNA levels (Figure 1C). Reads were first aligned to mature
143 tRNA sequences, which contained predicted tRNA genes from tRNAscan-SE (31, 32) modified
144 by intron removal and the addition of mature –CCA 3' ends, yielding counts for mature tRNAs
145 (Figure 2A). The remaining reads were aligned to a masked genome appended with pre-tRNA
146 sequences including intact introns and 50 nt of upstream and downstream flanking sequence.
147 Thus, classification as a pre-tRNA required the absence of a 3' –CCA and the presence of 5'
148 leader, intron, or 3' trailer sequence.
149 tRNAscan-SE yields a list of genes containing both true tRNAs and tRNA-like sequences
150 such as pseudo-tRNAs and B2 SINE elements. Among these, we focused on the high
151 confidence set of tRNA genes as defined by the genomic tRNA database (n=405) (31, 32). Due
152 to unique genomic sequences found in 5' leader and 3' trailers, pre-tRNA reads were less likely
153 to multimap to the genome and were used as a proxy for expression of the respective tRNA
154 genes. Of the 405 predicted high confidence tRNA genes, we were able to map pre-tRNAs
155 originating from 313 tRNA genes using Salmon (Supplemental File 1) (33). Additionally, we
156 used a different mapping strategy analyzing only the uniquely mapping reads in order to more
157 confidently identify the locus of origin for expressed pre-tRNAs, although this strategy may
158 underestimate the total number of expressed pre-tRNAs. Restricting the data to uniquely
159 mapping reads yielded a total of 244 tRNA genes with detectable pre-tRNAs from infected cells.
160

Figure 2

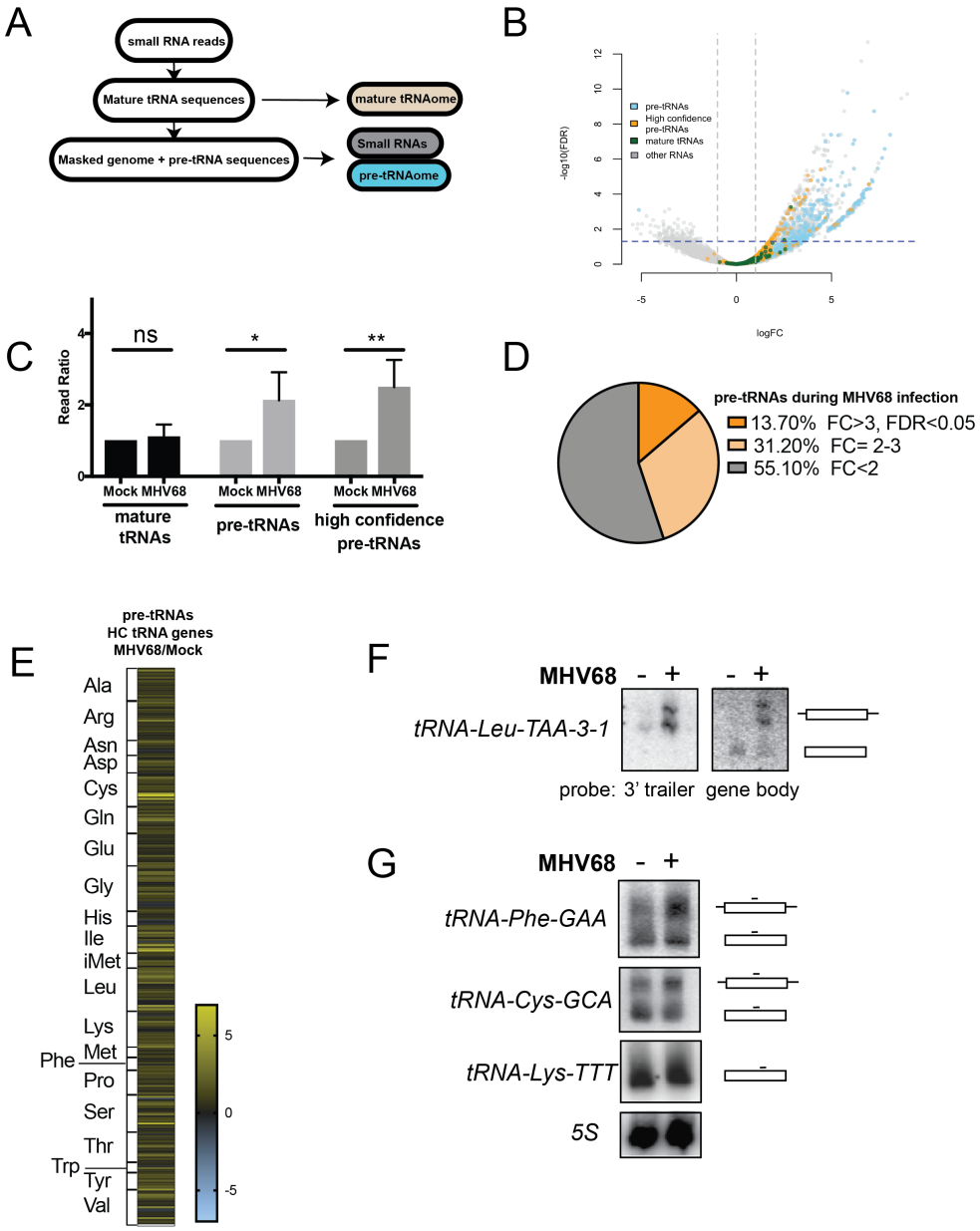

Figure 2. DM-tRNA-seq reveals differential expression of the pretRNAome upon infection.
(A) Reads from DM-tRNA-seq (MC57G +/- 24 h MHV68 infection) were aligned to mature tRNA sequences, generating the mature tRNAome. Other small RNAs and pre-tRNAs were mapped by aligning the remaining reads over the masked mm10 reference genome with appended pre-tRNA sequences. All tRNA sequences were predicted by tRNAscanSE. (B) Differential gene expression analysis from DM-tRNA-seq was plotted as fold change (FC) versus the false discovery rate (FDR). Pre-tRNAs (high confidence in yellow, other in blue), mature tRNAs (high confidence only in red), and other small RNA reads (gray) are annotated and the dotted lines represent the boundaries of FC=2 and FDR=0.05. High confidence refers to the tRNA gene set predicted by GtRNAdb. (C) Raw read counts for mature tRNAs, pre-tRNAs, or high confidence pre-tRNAs from DM-tRNA-seq of MHV68-infected MC57Gs were compared to those of uninfected cells. Error bars show SD and statistics were calculated using an unpaired t- test on raw read counts from four replicates. (D) A pie chart shows the percentage of high confidence pre-tRNAs detected by DM-tRNA-seq that were significantly upregulated (dark orange, FC>3 and FDR<0.05) versus upregulated but not significant (light orange, FC>2 and FDR>0.05) versus unregulated (gray, FC<2). (E) A heat map of log2FC changes of pre-tRNA levels by DM-tRNA-seq by isotype. (F) RNA from mock or MHV68-infected MC57Gs was used for northern blot using probes specific for either the 3' trailer or gene body of tRNA-Leu-TAA-3-1. (G) RNA from mock or MHV68-infected MC57Gs was used for northern blot using probes specific for the gene body of the tRNA-Phe-GAA, tRNA-Cys-GCA, and tRNA-Lys-TTT families. Probes detected tRNAs from multiple loci, and those for tRNA-Phe-GAA and tRNA-Cys-GCA also detected pre-tRNAs induced during infection. All infections were done in MC57G fibroblasts at an MOI=5 for 24 hours.

161
162

163 Differential gene expression analysis revealed that pre-tRNAs are more abundant during
164 MHV68 infection (Figure 2B, blue and orange circles). In fact, raw read count ratios alone (sum
165 of total reads per replicate compared to mock) displayed an increase in pre-tRNA reads present
166 in infected cells compared to uninfected cells (Figure 2C). It is likely that many of the highly
167 expressed pre-tRNA genes (Figure 2B, blue circles) that are not in the high confidence tRNA
168 gene list (Figure 2B, orange circles) are SINE retrotransposons, as B2 SINEs are robustly
169 induced during infection (20, 34). Focusing on high confidence tRNA genes, we found many of
170 these loci produce more pre-tRNAs during infection (Figure 2B, yellow circles; Figure 2C). Yet,
171 while total levels of pre-tRNAs were higher in infected cells, we observed selectivity in which
172 tRNA genes were upregulated. Of the high confidence pre-tRNAs detectably expressed in
173 uninfected MC57G cells, approximately one-fifth were significantly upregulated during MHV68
174 infection, depending on the mapping strategy used (Figure 2D shows results with Salmon: 43
175 out of 313 (13.7%), unique mappers: 63 out of 244 (25.8%), FDR<0.05). However, a general
176 trend of increased expression of pre-tRNAs was observed as judged by a fold change greater
177 than 2 (Figure 2D shows results with Salmon: 141 out of 314 (44.9%); unique mappers: 158 out
178 of 244 (64.8%)). In general, at least one member of each tRNA isotype (tRNAs encoding the
179 same amino acid) were present in the differential hits, but not all isodecoders (tRNAs with the
180 same anticodon) were represented (Figure 2E, Supplemental Figure 2). A triple A box motif that
181 is present in each RNAPIII-driven TMER locus encoded by MHV68 and in 10% of host tRNA
182 genes (35) was not enriched in the differential hits (Supplemental Figure 3).
183 Unlike pre-tRNAs, the levels of most mature tRNAs did not change in a statistically
184 significant manner, suggesting that the upregulated pre-tRNAs do not undergo canonical
185 maturation (Supplemental File 1). In fact, only two high confidence tRNA genes (tRNA-Lys-TTT-
186 2-2 and tRNA-Leu-TAA-3-1) showed significant differential expression at the level of the mature
187 tRNA transcript (Figure 2B, green circles FDR<0.05). To validate these findings, we designed
188 northern blot probes to the 3' trailer or gene body specific to transcripts originating from tRNA-

189 Leu-TAA-3-1 (Figure 2F). While pre-tRNA transcripts were elevated from the tRNA-Leu-TAA-3-1
190 gene in infected cells, levels of mature tRNAs did not change upon infection. We were not able
191 to design a probe specific for tRNA-Lys-TTT-2-2 transcripts, but using a probe that recognizes
192 members of the tRNA-Lys-TTT family did not show any differences in mature tRNA-Lys-TTT
193 expression during MHV68 infection (Figure 2G). Similarly, other tRNA families that we tested by
194 northern blotting, including tRNA-Phe-GAA and tRNA-Cys-GCA families, showed upregulation
195 at the level of the full-length pre-tRNA only (Figure 2G).
196
197 **RNA Polymerase III is recruited to upregulated tRNA genes during infection**
198 The distinct subset of tRNA genes that have higher expression at the pre-tRNA level during
199 MHV68 infection could be reflective of increased transcription, stability, or a combination of
200 both. To determine if the increase in pre-tRNA transcripts during infection results from
201 transcriptional upregulation, we performed chromatin immunoprecipitation followed by qPCR
202 (ChIP-qPCR) to measure occupancy of the RNAPIII subunit Polr3A at several loci in mock and
203 MHV68-infected MC57G fibroblasts. RNAPIII abundance specifically increased during MHV68
204 infection at each of the tested differentially expressed loci (tRNA-Tyr-GTA-1-3, tRNA-Leu-CAA-
205 1-1, and tRNA-Leu-TAA-3-1) but remained unchanged at a tRNA gene not differentially
206 expressed (tRNA-Ile-TAT-2-3) and at 7SK (Figure 3A). RNAPIII abundance at the RNAPII-
207 dependent GAPDH promoter was included as a negative control to show specificity of the
208 RNAPIII ChIP signal. These data suggest that there is an increase in RNAPIII recruitment to
209 select tRNA genes during MHV68 infection.
210 Maf1 is a well-studied negative regulator of transcription by RNAPIII whose activity is
211 controlled by phosphorylation and cellular localization in response to nutrients and stress
212 conditions (36, 37). When active, Maf1 directly targets the Brf1 subunit of TFIIIB and RNAPIII to
213 inhibit transcription. In addition, in proliferating and differentiated mammalian cells, Maf1

Figure 3

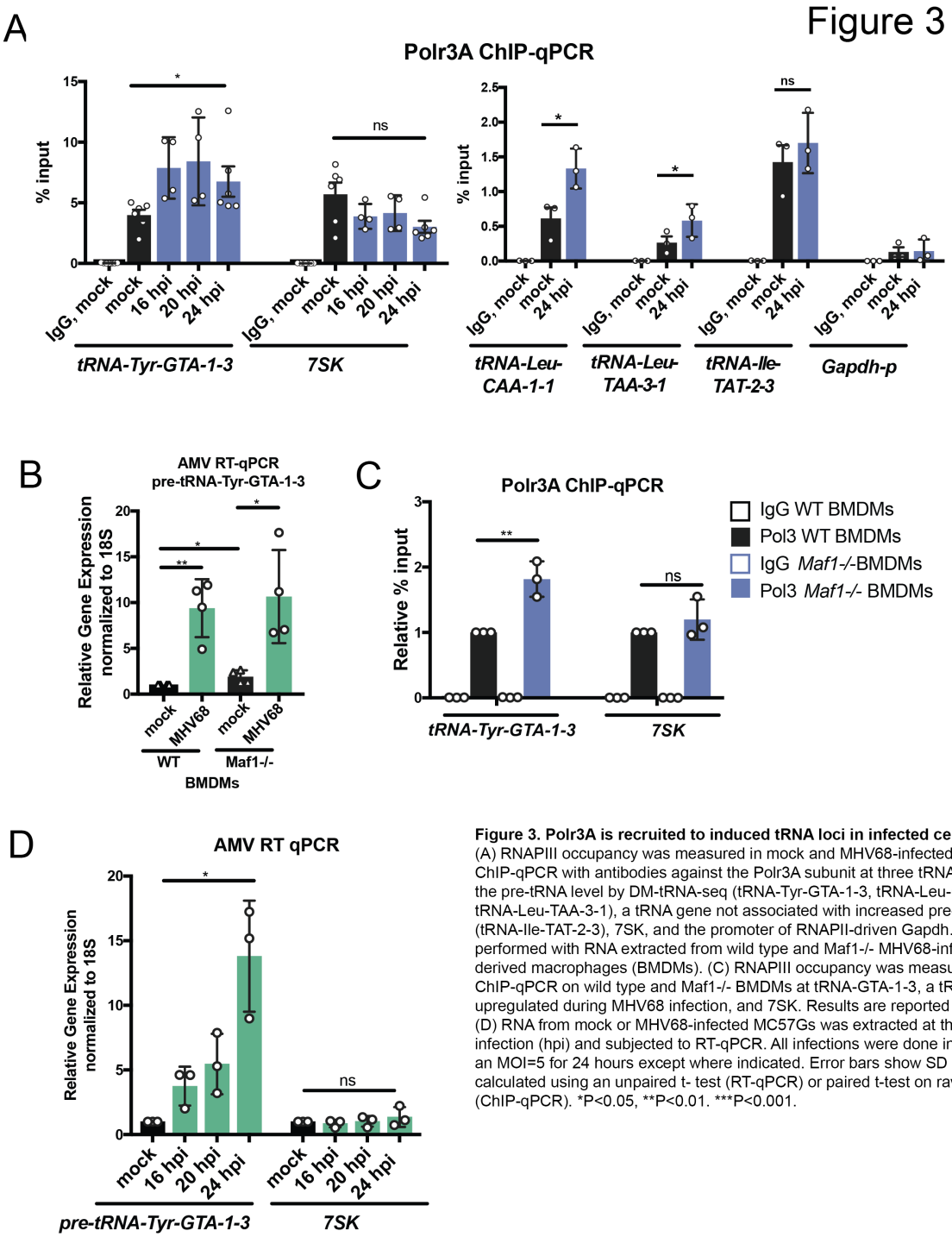

Figure 3. Polr3A is recruited to induced tRNA loci in infected cells.
(A) RNAPIII occupancy was measured in mock and MHV68-infected MC57Gs using ChIP-qPCR with antibodies against the Polr3A subunit at three tRNA genes upregulated at the pre-tRNA level by DM-tRNA-seq (tRNA-Tyr-GTA-1-3, tRNA-Leu-CAA-1-1, tRNA-Leu-TAA-3-1), a tRNA gene not associated with increased pre-tRNA levels (tRNA-Ile-TAT-2-3), 7SK, and the promoter of RNAPII-driven Gapdh. (B) RT-qPCR was performed with RNA extracted from wild type and Maf1-/- MHV68-infected bone marrow derived macrophages (BMDMs). (C) RNAPIII occupancy was measured using Polr3A ChIP-qPCR on wild type and Maf1-/- BMDMs at tRNA-GTA-1-3, a tRNA gene also upregulated during MHV68 infection, and 7SK. Results are reported in relative % input. (D) RNA from mock or MHV68-infected MC57Gs was extracted at the indicated hours post infection (hpi) and subjected to RT-qPCR. All infections were done in MC57G fibroblasts at an MOI=5 for 24 hours except where indicated. Error bars show SD and statistics were calculated using an unpaired t- test (RT-qPCR) or paired t-test on raw % input values (ChIP-qPCR). *P<0.05, **P<0.01. ***P<0.001.

215 chronically represses RNAPIII transcription to balance RNA synthesis with cellular demand (38,
216 39).

217 Thus, if the mechanism underlying MHV68 induction of pre-tRNAs involved antagonizing
218 Maf1-dependent repression, we reasoned that cells lacking Maf1 should no longer display a
219 difference in pre-tRNA levels between uninfected and infected cells. To test this hypothesis, we
220 derived primary bone marrow macrophages (BMDM) from WT and *Maf1-/-* mice and infected
221 them with MHV68 at an MOI=5. MHV68 infection of BMDMs resulted in ~10-fold increase in pre-
222 tRNA-Tyr upon MHV68 infection, demonstrating that increased pre-tRNA expression during
223 infection occurs in primary cells and is not unique to fibroblast cell lines (Figure 3B). MHV68-
224 infected WT and *Maf1-/-* BMDMs showed similar levels of pre-tRNA expression, indicating that
225 viral induction of pre-tRNA-Tyr levels was not dependent on *Maf1* regulation of RNAPIII. Similar
226 to other published reports (40), uninfected *Maf1*-/- cells showed a ~2-fold increase in pre-tRNA-
227 Tyr compared to WT BMDMs as well as increased RNAPIII promoter occupancy in ChIP
228 assays, confirming that RNAPIII activity is elevated in the absence of this negative regulator
229 (Figure 3B, 3C).

230 Even though the relative increases in pre-tRNA-Tyr levels were dramatically larger in
231 MHV68-infected cells compared to cells lacking Maf1 (Figure 3B,D), we were struck that the
232 increase in RNAPIII occupancy in these two scenarios was comparable (Figure 3A,C). To
233 explore the contribution of RNAPIII recruitment to pre-tRNA levels, we compared pre-tRNA
234 abundance by RT-qPCR (Figure 3D) and RNAPIII promoter occupancy by Polr3A ChIP-qPCR
235 (Figure 3A) across a time course of MHV68 infection in MC57G fibroblasts. Pre-tRNA-Tyr levels
236 were induced about 5-fold at 16 and 20 hpi but increased to a nearly 15-fold induction at 24 hpi,
237 whereas *7SK* levels remained constant (Figure 3D). In contrast to the RNA abundance data,
238 RNAPIII occupancy at the pre-tRNA-Tyr promoter was modestly increased by 16hpi, but did not
239 further increase at later time points (Figure 3A). Thus, after 16 hpi, it is likely that post-
240 transcriptional mechanisms underlie the continued accumulation of pre-tRNA-Tyr.

241 **Virus-induced mRNA degradation contributes to post-transcriptional accumulation of**
242 **pre-tRNAs**

243 We reasoned that selective post-transcriptional accumulation of pre-tRNAs might occur if
244 pre-tRNA maturation or turnover were impaired, for example if the virus down-regulated factors
245 involved in these processes. A well-characterized phenotype of MHV68 infection is the
246 widespread degradation of host mRNAs, which is caused by the viral mRNA-specific
247 endonuclease muSOX (28). Notably, the levels of the RNAPIII-transcribed viral tRNAs (vtRNAs)
248 are decreased in cells infected with the MHV68 muSOX point mutant R443I (MHV68.R443I),
249 which has reduced host shutoff activity (41). muSOX is expressed with early kinetics, but its
250 mRNA depletion phenotype is most prominent at late stages of infection, coincident with
251 maximal pre-tRNA accumulation. We tested whether virus-induced mRNA decay contributes to
252 post-transcriptional accumulation of cellular pre-tRNAs by measuring pre-tRNA abundance in
253 MC57G cells infected with MHV68.R443I or the mutant revertant (MR) virus in which the R443I
254 was restored to wild type (Figure 4A). Similar to the vtRNAs, the levels of cellular pre-tRNA-Tyr
255 and pre-tRNA-Leu were lower levels in cells infected with the R443I mutant compared to MR
256 MHV68 (Figure 4A). In contrast, the viral ORF50 mRNA was slightly increased during the R443I
257 mutant infection, consistent with previous reports (41). To determine if these changes reflected
258 transcriptional output, we measured RNAPIII binding at two differentially regulated host tRNA
259 genes and the viral TMER2 locus during MR vs R443I infection (Figure 4B). RNAPIII abundance
260 was similar during infection with MR and R443I viruses, in stark contrast to the difference in pre-
261 tRNA and vtRNA transcript abundance. This result suggests that the decreased abundance of
262 these transcripts in total RNA is not due to decreased levels of transcription. Collectively, these
263 data suggest that the mRNA decay phenotype associated with WT MHV68 infection is not
264 involved in transcriptional activation of tRNA loci, but instead stabilizes the unprocessed pre-
265 tRNAs.

Figure 4

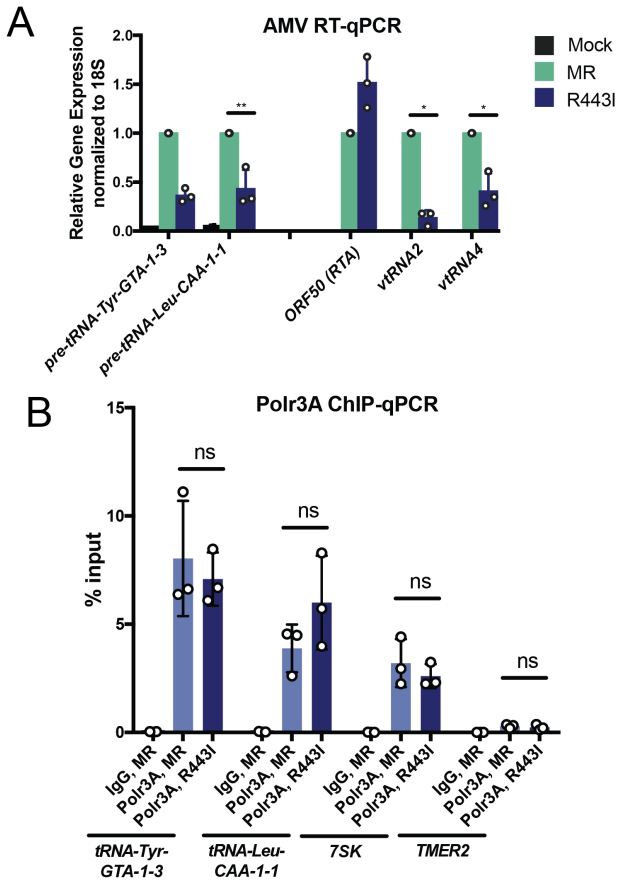

Figure 4. muSOX activity is required for pre-tRNA accumulation, but not for RNAPIII recruitment.
(A) MC57Gs were infected with muSOX R443I or mutant revertant (MR) MHV68 and RT-qPCR was performed with extracted RNA. (B) RNAPIII occupancy was measured using ChIP-qPCR with antibodies against the Polr3A subunit of RNAPIII at induced tRNA loci, viral TMER2, and 7SK using the cells described in (A). All infections were done at an MOI=5 for 24 hours. Error bars show SD and statistics were calculated using an unpaired t- test (RT-qPCR) or paired t-test on raw % input values (ChIP-qPCR). *P<0.05, **P<0.01. ***P<0.001.

266

267

268 **Discussion**

269 This study represents the first genome-wide analysis of how infection modulates the
270 tRNAome, revealing that the model gammaherpesvirus MHV68 causes extensive changes to
271 pre-tRNA but not mature tRNA abundance. We did not detect increased expression across all
272 tRNA genes, but instead found a dramatic accumulation of pre-tRNAs from a subset of loci,
273 which may reflect differences in promoter accessibility, regulation and/or pre-tRNA processing.
274 Collectively, our data support a model whereby pre-tRNA accumulation during MHV68 infection

275 is driven by both RNAPIII recruitment and RNA stabilization (Figure 5). We hypothesize that
276 early events in infection stimulate RNAPIII-driven transcription of specific tRNA loci, while
277 muSOX-induced depletion or relocalization of pre-tRNA processing machinery stalls further
278 canonical processing of these transcripts, leading to their build up late in infection (Figure 5).
279 These findings are bolstered by early reports showing enhanced RNAPIII activity during DNA
280 virus infection, including for select tRNAs (12-17, 27), suggesting that manipulation of the pre-
281 tRNA landscape is likely to be a conserved feature of numerous viruses.
282

Figure 5

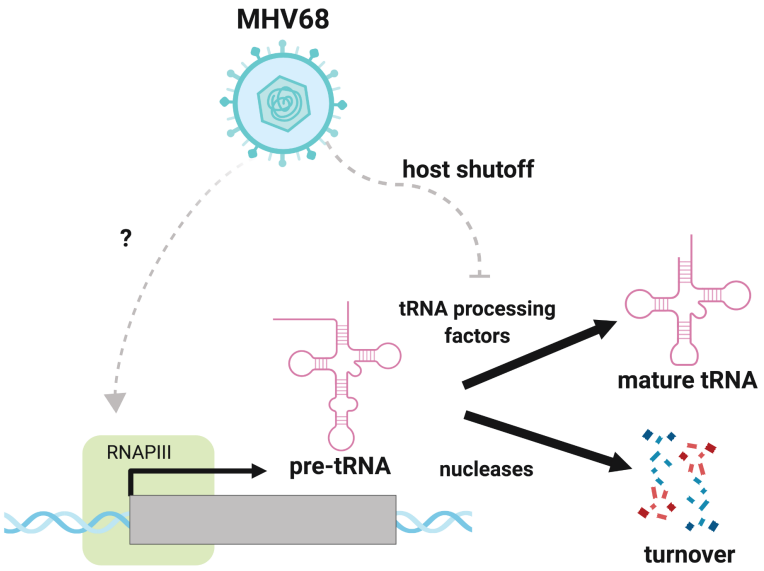

Figure 5. MHV68 infection induces pre-tRNA accumulation by transcriptional and post-transcriptional mechanisms. RNAPIII is recruited to specific tRNA genes by a Maf1-independent mechanism, increasing the output of pre-tRNAs. Pre-tRNAs accumulate in infected cells due to depletion of maturation or turnover machinery during muSOX-mediated mRNA decay (host shutoff).

283
284 Pre-tRNA steady state levels are dependent on both the production and stability of the
285 pre-tRNA transcripts. We performed Polr3A ChIP-qPCR and found that, for several tRNA
286 genes, increased pre-tRNA abundance was associated with higher levels of Polr3A occupancy
287 during infection. In contrast, a tRNA gene with constant pre-tRNA expression did not show

288 changes in Polr3A binding. This confirms that transcriptional increases- at least at some tRNA
289 genes- contribute to pre-tRNA accumulation during infection. Whether this is true for all tRNA
290 genes associated with increased pre-tRNA levels remains to be determined. Additionally,
291 increased RNAPIII occupancy during infection suggests a mechanism involving RNAPIII
292 recruitment to specific tRNA genes, and raises the possibility that these tRNA genes are not
293 expressed to their full potential in uninfected cell populations. In support of this, there is
294 considerable overlap between tRNA genes upregulated during MHV68 infection with those
295 upregulated in cells lacking Maf1, a negative regulator of RNAPIII that prevents polymerase
296 recruitment (59 of 79 pre-tRNAs induced by MHV68 infection of MC57G fibroblasts were also
297 increased in *Maf1-/-* versus WT liver in (40)). However, Maf1 does not appear to play a pivotal
298 role in pre-tRNA accumulation during MHV68 infection.

299 The mechanisms employed during MHV68 infection to increase RNAPIII recruitment
300 have not been identified. During EBV infection, TFIIIC subunit and Bdp1 protein levels increase,
301 along with transcripts for RNAPIII genes with type I and II promoters (*7SL*, *5S*, tRNAs), but not
302 those with type III promoters (*7SK*, *U6*, *MRP*) (12). In contrast, MHV68 infection leads to
303 transcriptional induction of B1/B2 SINEs (20, 34) and certain tRNA genes, all of which have type
304 II promoters. TFIIIB/C subunit mRNA levels do not increase during MHV68 infection, and
305 quantitative mass spectrometry of MHV68-infected cells indicates that total TFIIIB/C protein
306 levels are not elevated, although there may be enrichment of these factors in the nucleus (42).
307 Thus, RNAPIII regulation during MHV68 infection appears distinct from that observed with EBV
308 and may therefore involve novel mechanisms. Like EBV, SV40 infection leads to increased
309 TFIIIC protein levels, but additionally results in higher availability of TFIIIB by large T-antigen
310 sequestration of the retinoblastoma tumor suppressor protein (RB), a negative regulator of
311 RNAPIII transcription (43). The changes in RNAPIII output in mouse fibroblasts are similar
312 between SV40 and MHV68 infections (B1/B2 SINEs and certain tRNAs are induced (27, 44)),
313 plus mass spectrometry data suggests that RB subcellular concentration changes during

314 MHV68 infection (42). Thus, future studies will explore how RB is regulated during MHV68
315 infection and whether this protein is an important player in gammaherpesvirus-induced RNAPIII
316 activation. These could include the posttranslational regulation of transcription factor activities,
317 altered factor availability or epigenetic changes influencing gene accessibility.

318 With the exception of selenocysteine tRNA (7), all tRNAs genes use the same internal
319 A/B box promoter architecture for transcription. However, based on differential binding of
320 RNAPIII, many studies have revealed that tRNA genes are not equally transcribed in
321 mammalian cells, as measured by the differential binding of RNAPIII (7-9). Genome-wide
322 studies examining chromatin accessibility, modification and transcription factor binding have
323 suggested that a driver of RNAPIII occupancy at tRNA genes is open and active chromatin,
324 typically in the vicinity of RNAPII transcription sites, yet the basis for differential RNAPIII binding
325 remains to be determined. (7, 8, 45, 46). Further studies are also needed to assess how host
326 chromatin accessibility and modifications change during MHV68 infection. Interestingly, MHV68
327 infection leads to depletion of RNAPII-specific subunits, resulting in less RNAPII transcription of
328 the host genome during infection (42). There is some evidence of transcriptional interference
329 between RNAPIII and RNAPII bound at nearby genes, as depletion of the Rbp1 subunit of
330 RNAPII leads to upregulation of a subset of tRNA genes (47). It is possible that depletion of
331 RNAPII allows for increased recruitment of RNAPIII machinery. We hypothesize that a
332 combination of genome accessibility and transcription factor availability are associated with
333 tRNA transcriptional increases during infection.

334 Although tRNA gene transcription is elevated due to RNAPIII recruitment, the magnitude
335 of pre-tRNA abundance is unlikely to be explained by transcriptional activation alone. Instead,
336 our data suggest that pre-tRNA stability is also increased. While we have not been able to
337 measure pre-tRNA half-life directly (due to difficulty in robustly inhibiting RNAPIII in the required
338 short time frame of pre-tRNA processing), it is clear that pre-tRNAs accumulate dramatically
339 between 20-24 hpi, a time frame in which RNAPIII occupancy is unchanged. Infection-induced

340 pre-tRNAs do not seem to be processed into mature tRNAs, as we found no evidence of
341 differential expression at the mature tRNA transcript level. Similarly, *Maf1-/-* tissues exhibit
342 upregulation of pre-tRNAs without significant changes to mature tRNA levels, suggestive of a
343 homeostatic mechanism to maintain the size of mature tRNA pools when tRNA gene
344 transcription is increased (40). In both of these cases, it is possible that the increase of pre-
345 tRNAs upon transcriptional induction saturates processing machinery, an outcome well
346 established in yeast (48, 49), resulting in their clearance (degradation) from cells. It was striking
347 that some pre-tRNA transcripts revealed in our study were much more highly expressed than
348 others. These pre-tRNAs might have specific modifications, unique structural characteristics, or
349 processing fates that render them inherently more stable in the cell or during infection. Knowing
350 the identity of these potentially hyper-stable pre-tRNAs will help guide studies to investigate
351 unique features and broaden our understanding of tRNA maturation and turnover.

352 We hypothesized that tRNA processing and turnover machinery might be depleted in
353 infected cells due to gammaherpesvirus-induced host shutoff implemented at late stages of viral
354 infection. Widespread mRNA decay is initiated by a gammaherpesvirus-encoded endonuclease,
355 called SOX in KSHV and muSOX in MHV68. SOX and its homologs cleave RNAPII-transcribed
356 mRNAs, leading to subsequent downregulation of host protein synthesis (28, 50). Depletion of
357 host proteins might further increase the ratio of pre-tRNA to available processing and turnover
358 machinery, leading to increased pre-tRNA half-lives. Though total protein levels of tRNA
359 processing machinery are not dramatically altered during a 24-hour lytic infection cycle, there
360 are some decreases in nuclear abundance of tRNA-related factors during infection, including
361 the nuclear exosome (42). We hypothesize that modest abundance changes of many tRNA-
362 related processing and turnover complexes could have an additive effect on the stability of pre-
363 tRNAs in infected cells. Moreover, pre-tRNAs were less abundant in cells infected with the host
364 shut-off defective R443I virus, a phenotype not explained by changes in nascent pre-tRNA
365 levels or Polr3A abundance at tRNA genes. Viral TMER transcripts are also less abundant

366 under these conditions (41), suggesting that the factors involved with pre-tRNA stability during
367 infection may also be involved in viral TMER transcript stability. TMERs consist of a tRNA-like
368 sequence with 1-2 miRNA stem loops that are processed by the host tRNA 3' processing
369 enzyme tRNAse Z (51, 52). Whether tRNAse Z or other host factors are involved in stabilizing
370 host pre-tRNA and viral TMERs is an important question for the future.

371 Boosting RNAPIII activity is thought to promote the expression of RNAPIII-transcribed
372 genes encoded by some DNA viruses (e.g., Epstein-Barr virus EBERs, Adenoviruses VA RNAs,
373 MHV68 TMERs) -- however, not all DNA viruses encode RNAPIII genes, suggesting that
374 regulation of RNAPIII could be advantageous to the virus or host for other reasons. For
375 example, because nascent RNAPIII transcripts contain 5' triphosphate ends, they can and do
376 serve as substrates for RNA sensors in the cell, such as RIG-I (18, 19). These studies show that
377 while typically the 5' ends of RNAPIII transcripts are processed or protected from sensing by
378 protein binding partners, HSV-1 and KSHV infection tips the balance and results in exposure of
379 5' triphosphate ends of RNAPIII transcripts for RIG-I recognition. Additionally, increased tRNA
380 expression could contribute to tRNA fragmentation reported during viral infection and cancer;
381 there are increasing examples of these fragments functioning in gene regulation, cell
382 proliferation, and stress responses (5, 6). As DM-tRNA-seq is not optimized for analysis of tRNA
383 fragments, it is not yet clear if tRNA fragments are produced during MHV68 infection. However,
384 some tRNA fragments are processed from pre-tRNA transcripts, including pre-tRNA-Tyr (53,
385 54), and thus it would not be surprising if pre-tRNA-derived fragments also increased upon
386 infection. In summary, exploring viral modulation of host tRNAomes could lead to exciting
387 insights both for tRNA biology and for the role of RNAPIII activation during DNA virus infection.
388

389 **Materials and Methods**

390 **Cell and Virus Culture**

391 NIH3T3 and MC57G cell lines were obtained from ATCC, maintained in Dulbecco's modified
392 Eagle medium (DMEM; Gibco) supplemented with 10% fetal bovine serum (FBS; VWR), and
393 screened regularly for mycoplasma by PCR. Wild-type and *Maf1* knockout primary bone
394 marrow-derived macrophages (BMDMs) were differentiated from adult 3-6 month old C57BL/6
395 mice (40). Provided femurs and tibia were ground in a sterile tissue-culture hood using a mortar
396 and pestle in DMEM before being passed through a 70 µm filter to remove debris. Cells were
397 differentiated in macrophage media + PenStrep (High glucose DMEM, 10% FBS, 10% MCSF,
398 1% PenStrep, 1% GlutaMax) for 7 days before being frozen for later use. After thaw, cells were
399 not subjected to any media containing antibiotics. MHV68 was amplified in NIH3T12 cells and
400 TCID50 was measured on NIH3T3s by limiting dilution. GFP-expressing wild type (55) and
401 GFP-expressing ΔHS (SOX R443I (56)) MHV68 viruses were incubated with cells for 1 hour at
402 an MOI of 5 to allow viral entry, and then the virus-containing media was removed and replaced
403 with fresh media. PAA was used at a concentration of 200 µg/ml and was added at the start of
404 the infection. UV-inactivation of MHV68 was performed by autocrosslinking twice in a
405 Stratalinker 2400 (1200uJX100). For infection of BMDMs, virus was added to cells in serum-free
406 DMEM for 4 hours in non-TC treated plates. Virus containing media was then aspirated and
407 replaced with macrophage media without antibiotics.
408
409 **RNA isolation and analysis**
410 Total RNA was isolated from cells using TRIzol (Invitrogen), treated with Turbo DNase (Ambion)
411 and reverse transcribed with AMV RT (Promega) primed with random 9-mers. For TGIRT-
412 qPCR, cDNA was synthesized with the TGIRT™-III Enzyme (InGex) following manufacturer's
413 instructions. Quantitative PCR analysis was performed with iTaq Universal SYBR Green
414 Supermix (Bio-Rad) using the primers listed in Table 1. qPCR is performed on at least three
415 biological replicates and Ct values were measured from three technical replicates per biological
416 sample. Fold change was calculated by ΔΔCT method. For northern blots, 20 µg of RNA was

417 loaded into 8% PAGE/7 M Urea gels, transferred to Hybond-XL (GE) membranes using a
418 Trans-blot Turbo Transfer system (Bio-Rad). Blots were pre-hybridized in ULTRAhyb buffer
419 (Thermo Fisher) at 42 °C for 1 hour before adding radiolabeled probe. Probes were generated
420 by end-labeling oligos listed in Table 1 using T4 PNK and [γ-^{32}P]-ATP. Blots were probed
421 overnight at 42 °C, washed 3 times for 5 minutes in 0.5x SSC and 0.1% SDS. Primer extension
422 was performed on 10 µg of RNA using a 5' fluorescein labeled oligo specific for B2 SINEs or
423 7SK. RNA was ethanol precipitated and resuspended in 9 µl of annealing buffer (10 mM Tris-
424 HCl, pH7.5, 0.3 M KCl, 1 mM EDTA) plus 1 µl of 5' fluorescein labeled oligo. Sample was briefly
425 heated to 95 °C, then incubated at 55 °C for 1 hour. 40 µl of extension buffer (10 mM Tris-HCl,
426 pH 8.8, 5 mM MgCl2, 5 mM DTT, 1 mM dNTP) and 1 µl of AMV RT (Promega) was added and
427 the sample was incubated at 42 °C for 1 hour. Nucleic acids were precipitated, resuspended in
428 RNA loading dye, and separated in 8% PAGE/ 7 M Urea gels.
429
430 **DM-tRNA-seq library preparation**
431 Protocol was modified from (3). His-tagged wild-type and D135S AlkB plasmids were obtained
432 from Addgene (#79050 and #79051) and proteins were purified by a Ni-NTA column followed by
433 cation exchange. Total RNA was spiked with *in vitro* transcribed *E. coli* tRNA-Lys, *E. coli* tRNA-
434 Tyr, and *S. cerevisiae* tRNA-Phe transcripts at 0.01 pmol IVT tRNAs per µg total RNA. RNA was
435 deacylated in 0.1M Tris-HCl, pH 9 at 37 °C for 45 min, ethanol purified, and then
436 dephosphorylated with PNK. Deacylated and dephosphorylated RNAs were then purified with a
437 mirVANA small RNA purification kit (Ambion) to isolate RNAs ≤ 200 nucleotides. Small RNAs
438 were demethylated in 300 mM NaCl, 50 mM MES pH 5, 2 mM $MgCl_2$, 50 µM ferrous ammonium
439 sulfate, 300 µM 2-ketoglutarate, 2 mM L-ascorbic acid, 50 µg/ml BSA, 1U/µl SUPERasin, 2X
440 molar ratio of wt AlkB, and 4X molar ratio of D135S AlkB for 2 hours at room temperature.
441 Reaction was quenched with 5 mM EDTA and purified with Trizol. 100 ng demethylated small

442 RNAs were used for library prep with a TGIRT Improved Modular Template-Switching RNA-seq
443 Kit (InGex) following the manufacturer's instructions. The included RNA/DNA heteroduplex for
444 the template switching reaction by TGIRT contains a 3' N-overhang on the DNA primer to
445 promote reverse transcription of all small RNAs (as opposed to the T-overhang for targeting
446 mature tRNAs described in (3)). PCR amplification was performed with Phusion polymerase
447 (Thermo Fisher) with Illumina multiplex and barcoded primers synthesized by IDT for 12 cycles.
448 Library was sequenced on a HiSeq4000. Data has been deposited at NCBI GEO, series
449 GSE142393.
450
451 **DM-tRNA-seq bioinformatic analysis**
452 tRNAscan-SE(57) was used to create the predicted tRNA gene library. Pre-tRNA sequences
453 were defined by adding 50bp of genomic sequences on 5' and 3' ends of the predicted tRNA
454 genes. Mature tRNAs were appended with a CCA tail and were clustered as described in (58).
455 Illumina 150bp paired-end sequence data were subjected to quality control using BBDuk
456 (https://jgi.doe.gov/data-and-tools/bbtools/). Sequencing adapters were removed from raw
457 reads. Bases that have quality score lower than 30 were trimmed. Any reads that are at least 50
458 bp in length after quality control were aligned to mature tRNA reference using end-to-end
459 mapping mode in Bowtie2 (59) (version 2.3.4.1). Reads that did not map to mature tRNAs were
460 then mapped to the masked mm10 genome appended with pre-tRNA sequences. Two
461 approaches were used for this mapping step. One is to use Bowtie2, with reads that map to
462 multiple locations excluded from downstream analysis, followed by quantification of expression
463 using SALMON (33). The other approach used SALMON to map the reads and quantify the
464 expression levels, which includes the reads that map to multiple locations in estimating the
465 expression levels. Raw counts were normalized using spike-in RNA species using R package
466 RUVSeq (60). A generalized linear model was built to test for differential expression for each
467 RNA species, using R package edgeR (61, 62).

468

469 **Chromatin immunoprecipitation**

470 Cells from a 10 cm dish were crosslinked in 1% formaldehyde in PBS for 5 min at room
471 temperature, quenched in 0.125 M glycine, and washed twice with PBS. Crosslinked cells were
472 lysed with 1 ml ChIP lysis buffer (50 mM HEPES pH 7.9, 140 mM NaCl, 1 mM EDTA, 10%
473 glycerol, 0.5% NP40, 0.25% Triton X-100) by rotation for 10 min. Nuclei were collected by
474 centrifugation at 1700 x g for 5 min at 4°C, washed once with ChIP shearing buffer (50 mM Tris
475 Cl, pH 7.5, 10 mM EDTA, 0.1% SDS), then resuspended in 1 ml of ChIP shearing buffer.
476 Chromatin was sheared for 8 minutes using a Covaris S220 Focused-ultrasonicator at 140
477 power, 5% duty cycle, 200 bursts / cycle. Chromatin was spun at 15,000 x g for 5 min at 4°C
478 and the pellet was discarded. 40 µg of chromatin was incubated with 10 µg rabbit polyclonal
479 anti-POLR3A (Abcam ab96328) or rabbit IgG (Southern Biotech) overnight. 30 µl of mixed
480 protein A and G dynabeads (Thermo Fisher) were added and tubes were rotated for 2 h at 4 °C.
481 Beads were washed with low salt immune complex (20 mM Tris pH 8.0, 1% Triton X-100, 2 mM
482 EDTA, 150 mM NaCl, 0.1% SDS), high salt immune complex (20 mM Tris pH 8.0, 1% Triton X-
483 100, 2 mM EDTA, 500 mM NaCl, 0.1% SDS), lithium chloride immune complex (10 mM Tris pH
484 8.0, 0.25 M LiCl, 1% NP-40, 1% Deoxycholic acid, 1 mM EDTA), and Tris-EDTA for 5 min each
485 at 4°C with rotation. DNA was eluted from the beads using 100 µl of elution buffer (150 mM
486 NaCl, 50 µg/ml proteinase K) and incubated at 50°C for 2 hr, then 65°C overnight. DNA was
487 purified using a Zymo Oligo Clean and Concentrator kit and used for qPCR analysis using the
488 primers listed in Table 1.

489

490 **Replicates and statistical analysis**

491 This work contains cell culture-based assays, where biological replicates are defined as
492 experiments performed on at least three distinct samples (cells maintained in different flasks).
493 Technical replicates are defined as experiments performed on the same biological sample at

494 least three times. The datapoint for each biological replicate performed is depicted in the
495 Figures. Statistical analysis was performed using Prism 7 (Version 7.0c) software (GraphPad
496 Software), and the exact test performed is described in the Figure legends. The criteria for
497 including data involved the quality of the data for positive and negative controls.
498
499
500 **Table 1. Primers used in this study.**

Primer extension oligos (mouse)	
B2_PXT	TACACTGTAGCTGTCTTCAGACA
7SK_PXT	GAGCTTGTTTGGAGGTTCT
RT-qPCR primers (mouse)	
Mm_pre-tRNA-Tyr-GTA-1-3_F	CCTTCGATAGCTCAGTTGGTAGAGC
Mm_pre-tRNA-Tyr-GTA-1-3_R	CTTCGAGCCGGATTCGAACCAGCGAC
Mm_pre-tRNA-Leu-CAA-1-1_F	CGCCAGACTCAAGCTATCGC
Mm_pre-tRNA-Leu-CAA-1-1_R	TGTCAGAAGTGGGATTCGAACC
7SK_F	CCCCTGCTAGAACCTCCAAAC
7SK_R	CACATGCAGCGCCTCATTT
U6_F	CGCTTCGGCAGCACATATAC
U6_R	AAAATATGGAACGCTTCACGA
5S_F	TCTCGTCTGATCTCGGAAGC
5S_R	AGCCTACAGCACCCGGTATT
7SL_F	ATCGGGTGTCCGCACTAAGTT
7SL_R	CAGCACGGGAGTTTTGACCT
GTF3C1_F	TTCACACACCGCTTTCAAG
GTF3C1_R	CTCCAGTAGGTAATCGGATCACA

GTF3C2_F	ACAGCAAGAGGCGCTAAAAGG
GTF3C2_R	GGACTGATCTAAGAGACCAGGAA
GTF3C3_F	ATGGGGTGAGTAAGTCAGTTCCA
GTF3C3_R	TCCAACACAAATACATCGCCTG
GTF3C4_F	CCCAATGCGGGGTTTCAAATA
GTF3C4_R	CTGCACAGTCAGGCGATTGT
GTF3C5_F	TTGGTGTGCGTGGAGTACC
GTF3C5_R	CCCAGGGTCTGTAGCATCT
GTF3C6_F	GCGTCTCCGAACGCTATGG
GTF3C6_R	CCTCTCCGTGTCAATTCCCA
BDP1_F	TGCTTCTTCTGAGATAGGGCA
BDP1_R	GAGGGCTTCTTTAGCAGCACT
RT-qPCR primers (MHV68)	
MHV68_orf50_F	GGCCGCAGACATTTAATGAC
MHV68_orf50_R	GCCTCAACTTCTCTGGATATGCC
MHV68_gB_F	GGCCCAAATTCAATTTGCCT
MHV68_gB_R	CCCTGGACAACTCCTCAAGC
MHV68_vtRNA2_F	GGTAGAGCAGCGGTTCCT
MHV68_vtRNA2_R	ACTCCCCCTCTCAACCA
MHV68_vtRNA4_F	AGCGGCAGGCTCATC
MHV68_vtRNA4_R	ATCTCAACTCTGCGTCGG
ChIP-qPCR primers (mouse)	
Mm_tRNA-Tyr-GTA-1-3_F	CCTTCGATAGCTCAGTTGGTAGAGC
Mm_tRNA-Tyr-GTA-1-3_R	CTTCGAGCCGGATTCGAACCAGCGAC
Mm_tRNA-Leu-CAA-1-1_F	CGCCAGACTCAAGCTATCGC

Mm_tRNA-Leu-CAA-1-1_R	TGTCAGAAGTGGGATTCGAACC
Mm_tRNA-Leu-TAA-3-1_F	ACTGGGATGGCTGAGTGGTTAAGGC
Mm_tRNA-Leu-TAA-3-1_R	GCAGACAGTCGAGCAGTACA
Mm_tRNA-Ile-TAT-2-3_F	GCTCCAGTGGCGCAATCGGTTAGC
Mm_tRNA-Ile-TAT-2-3_R	GCCTAGCTCCAAAAGGATCG
7SK_F	CCCCTGCTAGAACCTCCAAAC
7SK_R	CACATGCAGCGCCTCATTT
GAPDH_promoter_F	GGTTATCACCAGGCCAGCTA
GAPDH_promoter_R	GGAAGGGAGAAAAGGCATTC
ChIP-qPCR primers (MHV68)	
MHV68_vtRNA2_F (TMER2)	GGTAGAGCAGCGGTTCCT
MHV68_vtRNA2_R (TMER2)	ACTCCCCCTCTCAACCA

501

502 **Supplemental File 1. Differential gene expression analysis output from DM-tRNA-seq**
503 **comparing MHV68-infected vs mock-infected MC57G fibroblasts.**

504

505 **Acknowledgements**

506 We thank Jie Li and the UC Davis Bioinformatics Core for valuable assistance with the
507 bioinformatics analysis and Ella Hartenian for providing samples. We thank members of the
508 Glaunsinger lab and Coscoy lab for discussion and comments on the manuscript. This research
509 was supported by an American Cancer Society Postdoctoral Award 131370-PF-17-245-01-MPC
510 to JMT, and National Institutes of Health grants CA136367 and AI147183 to BG and GM120358
511 to IW. BG is an investigator of the Howard Hughes Medical Institute.

512

513 **Competing Interests**

None

Supplemental Figure 1

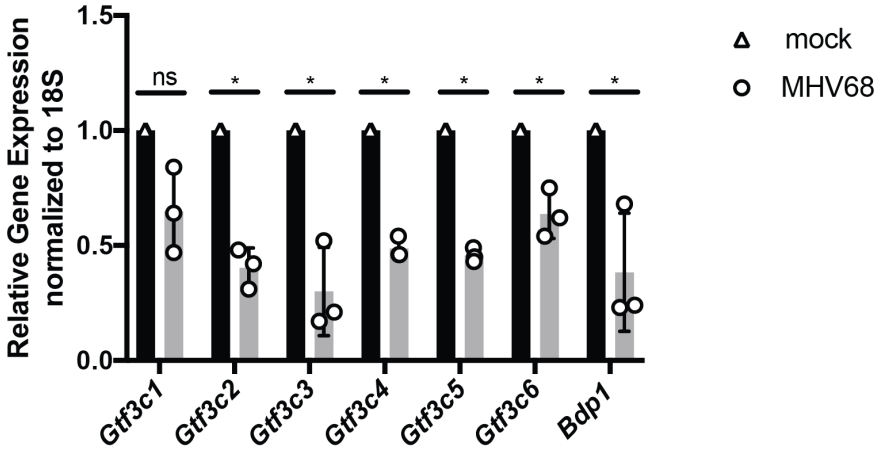

Supplemental Figure 1. The levels of mRNAs encoding TFIIIB and TFIIIC subunits are decreased upon MHV68 infection. RT-qPCR was performed on MC57Gs infected at an MOI=5 for 24 h and were done in triplicate. Error bars show SD and statistics were calculated using an unpaired t- test on raw ΔCt values. *P<0.05.

Supplemental Figure 2

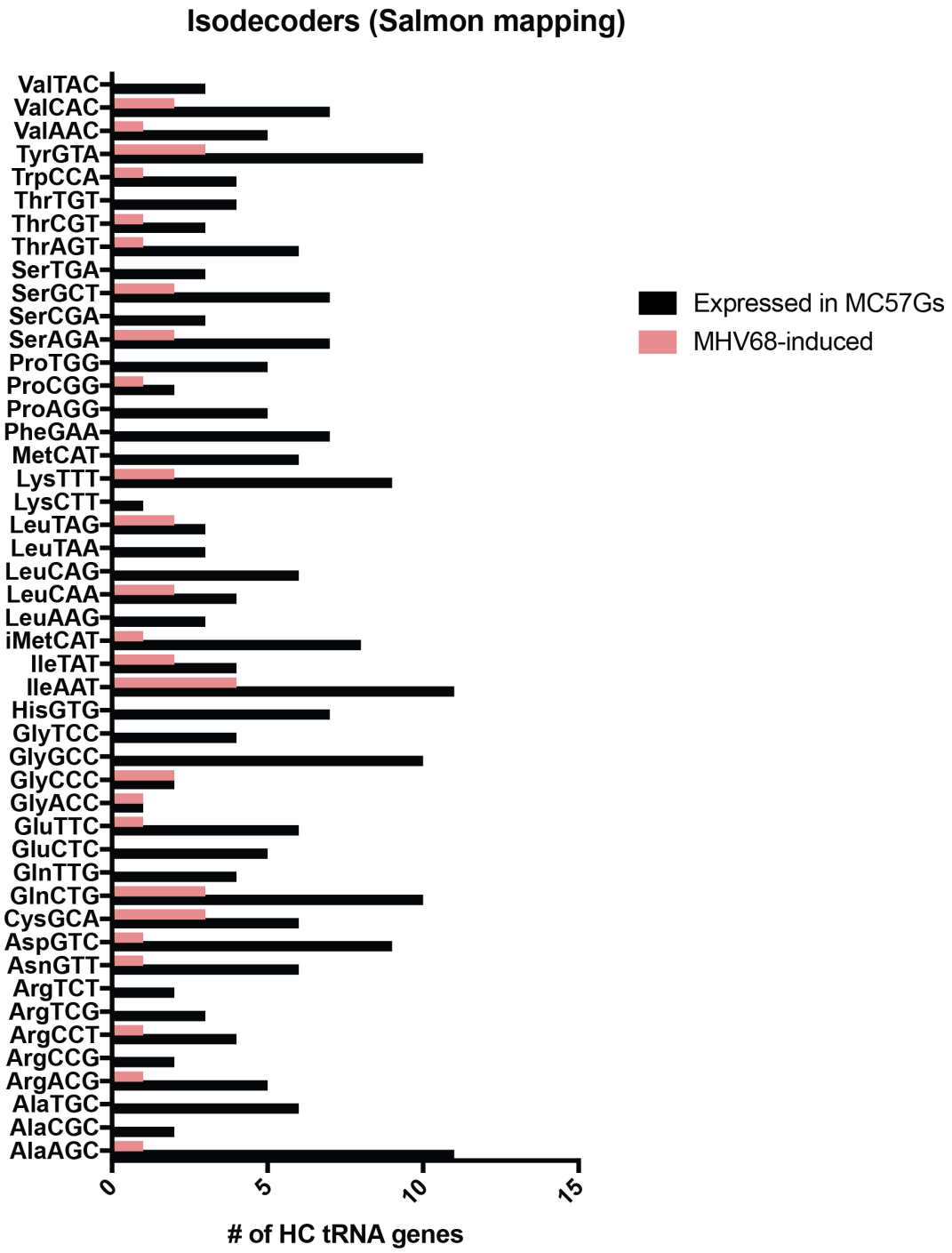

Supplemental Figure 2. A variety of tRNA isotypes are upregulated at the pre-tRNA level in response to MHV68 infection. Pre-tRNAs detected by DM-tRNA-seq from each tRNA isodecoder are shown in black, while the number with increased pre-tRNA expression in response to MHV68 are shown in are pink. Most isotypes (tRNAs encoding the same amino acid), but not all isodecoders (tRNAs with same anticodon), are represented.

Supplemental Figure 3

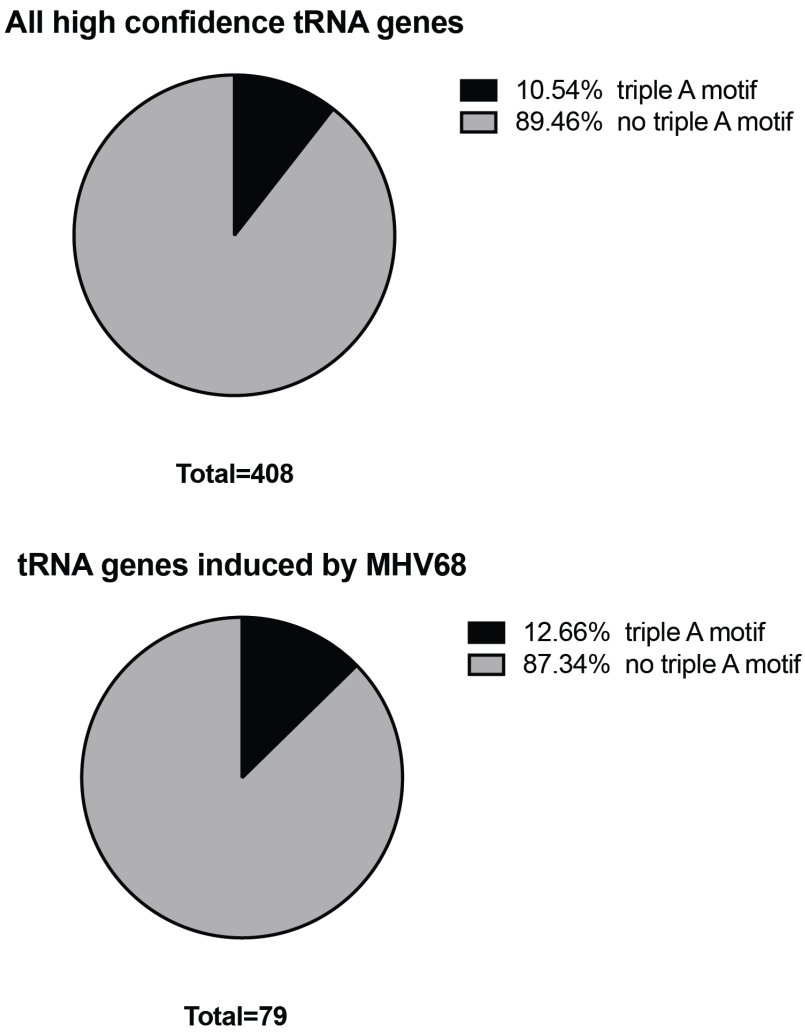

Supplemental Figure 3. A triple A-box motif is not enriched in MHV68-induced tRNA genes. The triple A-box motif (TRGYNNARNTGGTRGARNAGNNG) identified in MHV68 TMERs is present in ~11% of mouse high confidence tRNA genes as previously reported (35, 63). Both uniquely mapped and Salmon-identified MHV68-induced tRNA genes (n=79 genes) were analyzed for the triple A-box motif.

References

1. **Hoagland MB, Stephenson ML, Scott JF, Hecht LI, Zamecnik PC.** 1958. A soluble ribonucleic acid intermediate in protein synthesis. J Biol Chem **231:**241-257.
2. **Cozen AE, Quartley E, Holmes AD, Hrabeta-Robinson E, Phizicky EM, Lowe TM.** 2015. ARM-seq: AlkB-facilitated RNA methylation sequencing reveals a complex landscape of modified tRNA fragments. Nat Methods **12:**879-884.
3. **Zheng G, Qin Y, Clark WC, Dai Q, Yi C, He C, Lambowitz AM, Pan T.** 2015. Efficient and quantitative high-throughput tRNA sequencing. Nat Methods **12:**835-837.
4. **Gogakos T, Brown M, Garzia A, Meyer C, Hafner M, Tuschl T.** 2017. Characterizing Expression and Processing of Precursor and Mature Human tRNAs by Hydro-tRNAseq and PAR-CLIP. Cell Rep **20:**1463-1475.
5. **Oberbauer V, Schaefer MR.** 2018. tRNA-Derived Small RNAs: Biogenesis, Modification, Function and Potential Impact on Human Disease Development. Genes (Basel) **9**.
6. **Li S, Xu Z, Sheng J.** 2018. tRNA-Derived Small RNA: A Novel Regulatory Small Non-Coding RNA. Genes (Basel) **9**.
7. **Oler AJ, Alla RK, Roberts DN, Wong A, Hollenhorst PC, Chandler KJ, Cassiday PA, Nelson CA, Hagedorn CH, Graves BJ, Cairns BR.** 2010. Human RNA polymerase III transcriptomes and relationships to Pol II promoter chromatin and enhancer-binding factors. Nat Struct Mol Biol **17:**620-628.
8. **Raha D, Wang Z, Moqtaderi Z, Wu L, Zhong G, Gerstein M, Struhl K, Snyder M.** 2010. Close association of RNA polymerase II and many transcription factors with Pol III genes. Proc Natl Acad Sci U S A **107:**3639-3644.
9. **Canella D, Praz V, Reina JH, Cousin P, Hernandez N.** 2010. Defining the RNA polymerase III transcriptome: Genome-wide localization of the RNA polymerase III transcription machinery in human cells. Genome Res **20:**710-721.
10. **Li M, Kao E, Gao X, Sandig H, Limmer K, Pavon-Eternod M, Jones TE, Landry S, Pan T, Weitzman MD, David M.** 2012. Codon-usage-based inhibition of HIV protein synthesis by human schlafen 11. Nature **491:**125-128.
11. **Wang Q, Lee I, Ren J, Ajay SS, Lee YS, Bao X.** 2013. Identification and functional characterization of tRNA-derived RNA fragments (tRFs) in respiratory syncytial virus infection. Mol Ther **21:**368-379.
12. **Felton-Edkins ZA, Kondrashov A, Karali D, Fairley JA, Dawson CW, Arrand JR, Young LS, White RJ.** 2006. Epstein-Barr virus induces cellular transcription factors to allow active expression of EBER genes by RNA polymerase III. J Biol Chem **281:**33871-33880.
13. **Felton-Edkins ZA, White RJ.** 2002. Multiple mechanisms contribute to the activation of RNA polymerase III transcription in cells transformed by papovaviruses. J Biol Chem **277:**48182-48191.
14. **Gaynor RB, Feldman LT, Berk AJ.** 1985. Transcription of class III genes activated by viral immediate early proteins. Science **230:**447-450.
15. **Hoeffler WK, Roeder RG.** 1985. Enhancement of RNA polymerase III transcription by the E1A gene product of adenovirus. Cell **41:**955-963.
16. **Jang KL, Latchman DS.** 1989. HSV infection induces increased transcription of Alu repeated sequences by RNA polymerase III. FEBS Lett **258:**255-258.

564 17. **Panning B, Smiley JR.** 1994. Activation of RNA polymerase III transcription of human Alu
565 elements by herpes simplex virus. Virology **202:**408-417.
566 18. **Chiang JJ, Sparrer KMJ, van Gent M, Lassig C, Huang T, Osterrieder N, Hopfner KP, Gack**
567 **MU.** 2018. Viral unmasking of cellular 5S rRNA pseudogene transcripts induces RIG-I-
568 mediated immunity. Nat Immunol **19:**53-62.
569 19. **Zhao Y, Ye X, Dunker W, Song Y, Karijolich J.** 2018. RIG-I like receptor sensing of host
570 RNAs facilitates the cell-intrinsic immune response to KSHV infection. Nat Commun
571 **9:**4841.
572 20. **Karijolich J, Abernathy E, Glaunsinger BA.** 2015. Infection-Induced Retrotransposon-
573 Derived Noncoding RNAs Enhance Herpesviral Gene Expression via the NF-kappaB
574 Pathway. PLoS Pathog **11:**e1005260.
575 21. **Dong X, Feng H, Sun Q, Li H, Wu TT, Sun R, Tibbetts SA, Chen ZJ, Feng P.** 2010. Murine
576 gamma-herpesvirus 68 hijacks MAVS and IKKbeta to initiate lytic replication. PLoS
577 Pathog **6:**e1001001.
578 22. **Dong X, Feng P.** 2011. Murine gamma herpesvirus 68 hijacks MAVS and IKKbeta to
579 abrogate NFkappaB activation and antiviral cytokine production. PLoS Pathog
580 **7:**e1002336.
581 23. **Krug LT, Collins CM, Gargano LM, Speck SH.** 2009. NF-kappaB p50 plays distinct roles in
582 the establishment and control of murine gammaherpesvirus 68 latency. J Virol **83:**4732-
583 4748.
584 24. **Krug LT, Moser JM, Dickerson SM, Speck SH.** 2007. Inhibition of NF-kappaB activation in
585 vivo impairs establishment of gammaherpesvirus latency. PLoS Pathog **3:**e11.
586 25. **Tucker JM, Glaunsinger BA.** 2017. Host noncoding retrotransposons induced by DNA
587 viruses: a SINE of infection? J Virol doi:10.1128/JVI.00982-17.
588 26. **Schramm L, Hernandez N.** 2002. Recruitment of RNA polymerase III to its target
589 promoters. Genes Dev **16:**2593-2620.
590 27. **White RJ, Stott D, Rigby PW.** 1990. Regulation of RNA polymerase III transcription in
591 response to Simian virus 40 transformation. EMBO J **9:**3713-3721.
592 28. **Covarrubias S, Richner JM, Clyde K, Lee YJ, Glaunsinger BA.** 2009. Host shutoff is a
593 conserved phenotype of gammaherpesvirus infection and is orchestrated exclusively
594 from the cytoplasm. J Virol **83:**9554-9566.
595 29. **Torres AG, Pineyro D, Rodriguez-Escriba M, Camacho N, Reina O, Saint-Leger A,**
596 **Filonava L, Batlle E, Ribas de Pouplana L.** 2015. Inosine modifications in human tRNAs
597 are incorporated at the precursor tRNA level. Nucleic Acids Res **43:**5145-5157.
598 30. **Mohr S, Ghanem E, Smith W, Sheeter D, Qin Y, King O, Polioudakis D, Iyer VR, Hunicke-**
599 **Smith S, Swamy S, Kuersten S, Lambowitz AM.** 2013. Thermostable group II intron
600 reverse transcriptase fusion proteins and their use in cDNA synthesis and next-
601 generation RNA sequencing. RNA **19:**958-970.
602 31. **Chan PP, Lowe TM.** 2009. GtRNAdb: a database of transfer RNA genes detected in
603 genomic sequence. Nucleic Acids Res **37:**D93-97.
604 32. **Chan PP, Lowe TM.** 2016. GtRNAdb 2.0: an expanded database of transfer RNA genes
605 identified in complete and draft genomes. Nucleic Acids Res **44:**D184-189.
606 33. **Patro R, Duggal G, Love MI, Irizarry RA, Kingsford C.** 2017. Salmon provides fast and
607 bias-aware quantification of transcript expression. Nat Methods **14:**417-419.

608 34. **Karijolich J, Zhao Y, Alla R, Glaunsinger B.** 2017. Genome-wide mapping of infection-
609 induced SINE RNAs reveals a role in selective mRNA export. Nucleic Acids Res **45:**6194-
610 6208.
611 35. **Diebel KW, Claypool DJ, van Dyk LF.** 2014. A conserved RNA polymerase III promoter
612 required for gammaherpesvirus TMER transcription and microRNA processing. Gene
613 **544:**8-18.
614 36. **Graczyk D, Ciesla M, Boguta M.** 2018. Regulation of tRNA synthesis by the general
615 transcription factors of RNA polymerase III - TFIIIB and TFIIIC, and by the MAF1 protein.
616 Biochim Biophys Acta Gene Regul Mech **1861:**320-329.
617 37. **Willis IM, Moir RD.** 2018. Signaling to and from the RNA Polymerase III Transcription
618 and Processing Machinery. Annu Rev Biochem **87:**75-100.
619 38. **Orioli A, Praz V, Lhote P, Hernandez N.** 2016. Human MAF1 targets and represses active
620 RNA polymerase III genes by preventing recruitment rather than inducing long-term
621 transcriptional arrest. Genome Res **26:**624-635.
622 39. **Bonhoure N, Praz V, Moir RD, Willemin G, Mange F, Moret C, Willis IM, Hernandez N.**
623 2019. Chronic repression by MAF1 supports futile RNA cycling as a mechanism for
624 obesity resistance. bioRxiv doi:https://doi.org/10.1101/775353.
625 40. **Bonhoure N, Byrnes A, Moir RD, Hodroj W, Preitner F, Praz V, Marcelin G, Chua SC, Jr.,**
626 **Martinez-Lopez N, Singh R, Moullan N, Auwerx J, Willemin G, Shah H, Hartil K,**
627 **Vaitheesvaran B, Kurland I, Hernandez N, Willis IM.** 2015. Loss of the RNA polymerase
628 III repressor MAF1 confers obesity resistance. Genes Dev **29:**934-947.
629 41. **Abernathy E, Clyde K, Yeasmin R, Krug LT, Burlingame A, Coscoy L, Glaunsinger B.**
630 2014. Gammaherpesviral gene expression and virion composition are broadly controlled
631 by accelerated mRNA degradation. PLoS Pathog **10:**e1003882.
632 42. **Hartenian E, Glaunsinger B.** 2019. Herpesvirus infection reduces Pol II occupancy of
633 host promoters but spares viral promoters. bioRxiv doi:https://doi.org/10.1101/585984
634 .
635 43. **Larminie CG, Sutcliffe JE, Tosh K, Winter AG, Felton-Edkins ZA, White RJ.** 1999.
636 Activation of RNA polymerase III transcription in cells transformed by simian virus 40.
637 Mol Cell Biol **19:**4927-4934.
638 44. **Carey MF, Singh K, Botchan M, Cozzarelli NR.** 1986. Induction of specific transcription
639 by RNA polymerase III in transformed cells. Mol Cell Biol **6:**3068-3076.
640 45. **Barski A, Chepelev I, Liko D, Cuddapah S, Fleming AB, Birch J, Cui K, White RJ, Zhao K.**
641 2010. Pol II and its associated epigenetic marks are present at Pol III-transcribed
642 noncoding RNA genes. Nat Struct Mol Biol **17:**629-634.
643 46. **Yeganeh M, Praz V, Carmeli C, Villeneuve D, Rib L, Guex N, Herr W, Delorenzi M,**
644 **Hernandez N, Cycli Xc.** 2019. Differential regulation of RNA polymerase III genes during
645 liver regeneration. Nucleic Acids Res **47:**1786-1796.
646 47. **Gerber A, Ito K, Chu C, Roeder RG.** 2019. Induced RPB1 depletion reveals a direct gene-
647 specific control of RNA Polymerase III function by RNA Polymerase II. bioRxiv
648 doi:https://doi.org/10.1101/764605.
649 48. **Arimbasseri AG, Blewett NH, Iben JR, Lamichhane TN, Cherkasova V, Hafner M, Maraia**
650 **RJ.** 2015. RNA Polymerase III Output Is Functionally Linked to tRNA Dimethyl-G26
651 Modification. PLoS Genet **11:**e1005671.

652 49. **Karkusiewicz I, Turowski TW, Graczyk D, Towpik J, Dhungel N, Hopper AK, Boguta M.**
653 2011. Maf1 protein, repressor of RNA polymerase III, indirectly affects tRNA processing.
654 J Biol Chem **286:**39478-39488.
655 50. **Abernathy E, Glaunsinger B.** 2015. Emerging roles for RNA degradation in viral
656 replication and antiviral defense. Virology **479-480:**600-608.
657 51. **Pfeffer S, Sewer A, Lagos-Quintana M, Sheridan R, Sander C, Grasser FA, van Dyk LF,**
658 **Ho CK, Shuman S, Chien M, Russo JJ, Ju J, Randall G, Lindenbach BD, Rice CM, Simon V,**
659 **Ho DD, Zavolan M, Tuschl T.** 2005. Identification of microRNAs of the herpesvirus
660 family. Nat Methods **2:**269-276.
661 52. **Bogerd HP, Karnowski HW, Cai X, Shin J, Pohlers M, Cullen BR.** 2010. A mammalian
662 herpesvirus uses noncanonical expression and processing mechanisms to generate viral
663 MicroRNAs. Mol Cell **37:**135-142.
664 53. **Hanada T, Weitzer S, Mair B, Bernreuther C, Wainger BJ, Ichida J, Hanada R, Orthofer**
665 **M, Cronin SJ, Komnenovic V, Minis A, Sato F, Mimata H, Yoshimura A, Tamir I, Rainer J,**
666 **Kofler R, Yaron A, Eggan KC, Woolf CJ, Glatzel M, Herbst R, Martinez J, Penninger JM.**
667 2013. CLP1 links tRNA metabolism to progressive motor-neuron loss. Nature **495:**474-
668 480.
669 54. **Karaca E, Weitzer S, Pehlivan D, Shiraishi H, Gogakos T, Hanada T, Jhangiani SN,**
670 **Wiszniewski W, Withers M, Campbell IM, Erdin S, Isikay S, Franco LM, Gonzaga-**
671 **Jauregui C, Gambin T, Gelowani V, Hunter JV, Yesil G, Koparir E, Yilmaz S, Brown M,**
672 **Briskin D, Hafner M, Morozov P, Farazi TA, Bernreuther C, Glatzel M, Trattnig S, Friske**
673 **J, Kronnerwetter C, Bainbridge MN, Gezdirici A, Seven M, Muzny DM, Boerwinkle E,**
674 **Ozen M, Baylor Hopkins Center for Mendelian G, Clausen T, Tuschl T, Yuksel A, Hess A,**
675 **Gibbs RA, Martinez J, Penninger JM, Lupski JR.** 2014. Human CLP1 mutations alter tRNA
676 biogenesis, affecting both peripheral and central nervous system function. Cell **157:**636-
677 650.
678 55. **Adler H, Messerle M, Wagner M, Koszinowski UH.** 2000. Cloning and mutagenesis of
679 the murine gammaherpesvirus 68 genome as an infectious bacterial artificial
680 chromosome. J Virol **74:**6964-6974.
681 56. **Richner JM, Clyde K, Pezda AC, Cheng BY, Wang T, Kumar GR, Covarrubias S, Coscoy L,**
682 **Glaunsinger B.** 2011. Global mRNA degradation during lytic gammaherpesvirus infection
683 contributes to establishment of viral latency. PLoS Pathog **7:**e1002150.
684 57. **Lowe TM, Eddy SR.** 1997. tRNAscan-SE: a program for improved detection of transfer
685 RNA genes in genomic sequence. Nucleic Acids Res **25:**955-964.
686 58. **Hoffmann A, Fallmann J, Vilardo E, Morl M, Stadler PF, Amman F.** 2018. Accurate
687 mapping of tRNA reads. Bioinformatics **34:**2339.
688 59. **Langmead B, Salzberg SL.** 2012. Fast gapped-read alignment with Bowtie 2. Nat
689 Methods **9:**357-359.
690 60. **Risso D, Ngai J, Speed TP, Dudoit S.** 2014. Normalization of RNA-seq data using factor
691 analysis of control genes or samples. Nat Biotechnol **32:**896-902.
692 61. **Robinson MD, McCarthy DJ, Smyth GK.** 2010. edgeR: a Bioconductor package for
693 differential expression analysis of digital gene expression data. Bioinformatics **26:**139-
694 140.

695 62. **McCarthy DJ, Chen Y, Smyth GK.** 2012. Differential expression analysis of multifactor
696 RNA-Seq experiments with respect to biological variation. Nucleic Acids Res **40:**4288-
697 4297.
698